



# Hyperspectral Imaging for Earth Observation: Platforms and Instruments

Vaibhav Lodhi\*, Debashish Chakravarty and Pabitra Mitra

**Abstract** | Hyperspectral imaging is one of the promising remote sensing techniques. This technique records the spatial and spectral information of the object under study. Consequently, it has been gaining momentum in a number of Earth observing applications. The aim of this paper is to present the current trends of hyperspectral sensing from different platforms and instruments for various applications. For Earth observation, mobile platforms are discussed which include spaceborne, airborne, ground-based sensing, unmanned aerial system, and underwater vehicle-based. Under these different sensing platforms, hyperspectral imaging instruments are presented that have been developed by various public and private organizations in the past with some specific goals.

**Keywords:** *Hyperspectral imaging, Earth observation, Spaceborne, Airborne, Unmanned aerial system, Underwater vehicle*

## 1 Introduction

Spectral imaging techniques have been gaining popularity and provide spectral information of each pixel location of the image plane of the object under study. Multispectral, hyperspectral, and ultraspectral sensing are three main spectral imaging methods. Conceptually, there is no difference in between these methods. The difference lies in the number of images and spectral resolution within the spectral range. Hyperspectral imaging is the convergence of imaging and spectroscopy enables acquiring spatial and spectral distributions of the object under test. Consequently, this provides physical, chemical composition, and geometrical feature information. It consists hundreds or thousands of continuous spectral bands that generate a continuous spectral profile. Every material has its own unique spectral fingerprint. This enables us to identify material under test. Unlike hyperspectral imaging, multispectral generates a discrete spectral fingerprint of the material under test. Generally, it is assumed that the ultraspectral imaging has finer spectral resolution than hyperspectral imaging. Hyperspectral imaging is one of the most

widely used spectral imaging techniques. It has been used in a number of applications, including agriculture and food inspection<sup>1-4</sup>, biomedical applications<sup>5, 6</sup>, water resources<sup>7, 8</sup>, vegetation and forest<sup>9, 10</sup>, minerals detection and mapping<sup>11</sup>, surveillance and reconnaissance<sup>12</sup>, conservation of works of art<sup>13, 14</sup>, astronomy<sup>15</sup>, etc.

For Earth observation (EO) applications, hyperspectral imaging can be done using spaceborne, airborne, unmanned aerial system (UAS), underwater vehicle, and ground-based sensing platforms. The aim of this article was to discuss hyperspectral image acquisition by moving platforms along with presenting some of the major hyperspectral instruments developed by various space agencies, private and public organizations across the world for different working environments. In the proposed paper, we introduce a conceptual representation of hyperspectral imaging, together with components, descriptions, and sensor simulators.

Indian Institute  
of Technology Kharagpur,  
Kharagpur, India  
\* vaibhav.lodhi@gmail.  
com

## 2 Hyperspectral Remote Sensing

Conventionally, spectral remote sensing (multispectral) sensors such as Thematic Mapper (TM) and Enhanced Thematic Mapper (ETM)+ acquire spectral information in few discrete bands from visible to infrared range and their bandwidths are wider than 100 nm. Multispectral sensing system employs a small number of parallel sensor arrays to detect radiation of broad wavelength bands. In such a case, identification, detection, and discrimination capability decreases due to low spectral resolution. On the other hand, the hyperspectral imaging system collects data in narrow and more number of spectral bands as compared to the multispectral sensor. It consists of hundreds of spectral bands with a few nanometer spectral resolution, generates continuous spectral signature as compared to conventional spectral imaging (multispectral). The information content of hyperspectral images is much more than multispectral images. It has a great potential to detect differences among land and water and has a capability to discriminate individual absorption bands in mineral deposits and vegetation types. Examples of multispectral and hyperspectral signatures have been shown in Fig. 1. As shown in Fig. 1a and c, distinct materials may be discriminated easily by multispectral signature and

very easily by hyperspectral signature. However, in case of photosynthetic vegetation, i.e., spruce needle, lawn grass, maple leaf, and Russian olive multispectral data appear nearly identical, but it may be possible to separate using hyperspectral data due to minute spectral variations and number of absorption bands. Hyperspectral signature provides information about absorption depth and bands of the material. Absorbance bands may be used for identification, characterization, and abundance estimation purpose.

Initially, hyperspectral imaging is used for remote sensing purpose. Nowadays, it has been gaining popularity for industrial applications as well. In general, pushbroom technique is used for airborne, spaceborne and other platforms based on remote sensing to acquire hyperspectral data for Earth observation applications. Normally, it consists of fore-optics, slit, collimating optics, dispersive element (transmission grating), focusing optics, and detector array<sup>17</sup> as shown in Fig. 2. Fore-optics image the light onto the slit from the scene for data formation. After collimation, light passes from the grating and disperses into different wavelengths, and dispersed light is focussed onto the detector array. Slit dimension defines the pixel intervals to project light of different wavelengths along the column of a detector

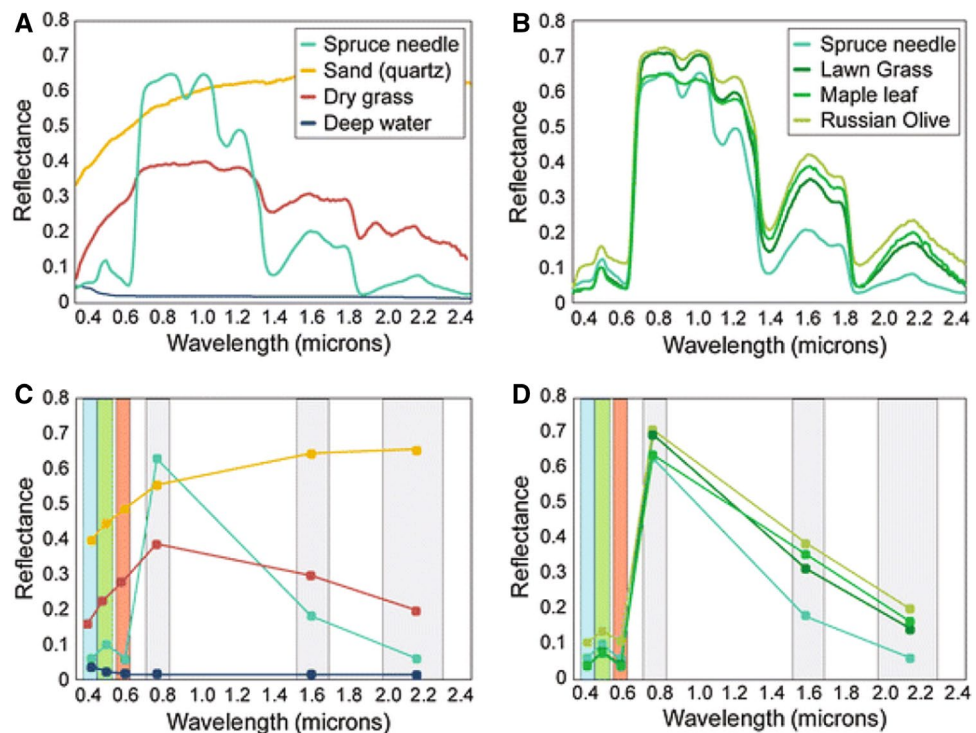


**Figure 1:** Example of multispectral and hyperspectral signatures<sup>10</sup>.

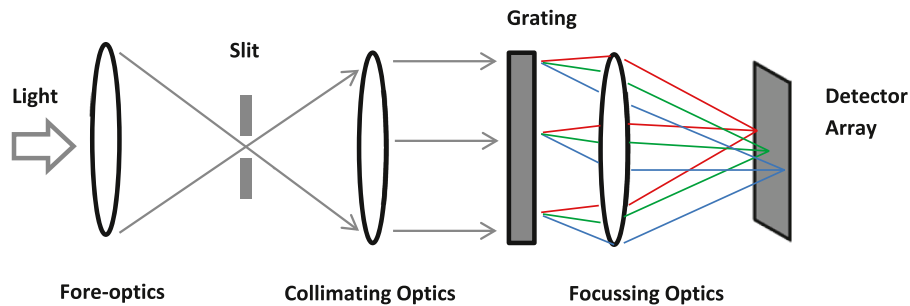


**Figure 2:** Schematic representation of the operation of hyperspectral imaging system.

array. In such a way, it forms spectral information in one direction and spatial information in other direction. Prism, grating and linear variable filter (LVF) may be used to achieve high spectral resolution in hyperspectral imaging.

### 3 Hyperspectral Imaging System

Hyperspectral imaging is one of the popular Geo-imaging techniques. Hyperspectral imaging system collects a number of images with narrow wavelength range, known as a spectral band. Combination of these spectral bands forms 3-Dimensional data known as hypercube

(known as a spectral cube, data cube, data volume and data cube). Hyperspectral data include two spatial dimensions and one spectral dimension to form the data cube. Hyperspectral imaging system is an advanced imaging system which includes all the basic components of an imaging system. Normally, they are lens assembly, an image sensor (Focal Plane Array), and image processor. However, a Focal plane array is a two-dimensional form. Therefore, in order to capture all three dimensions of the spectral cube, conventionally, requires either spatially or spectrally scanning mechanism. Nowadays, snapshot

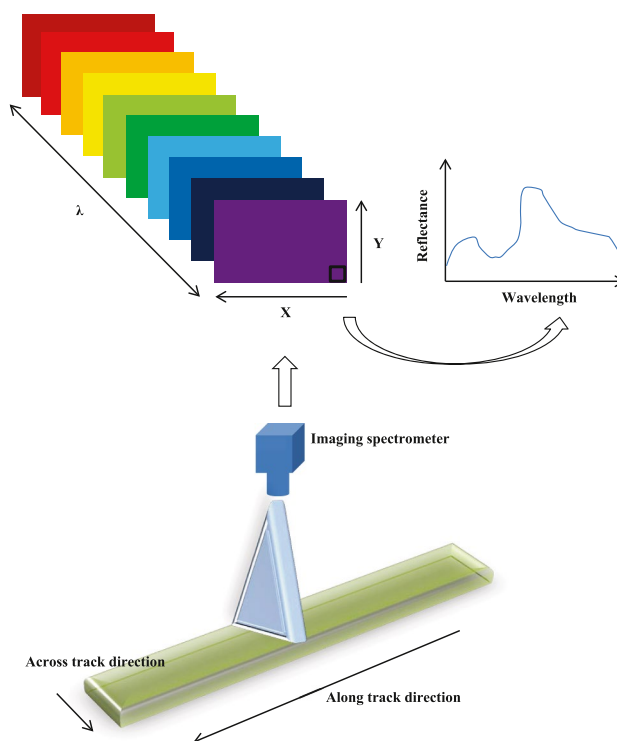


**Figure 3:** Conceptual representation of hyperspectral imaging for Earth observation.

spectral imaging system is also available which captures entire dataset during single detector integration period. However, this technique is not popular for Earth-observing applications.

For spatial scanning, either instrument or object under observation moves w.r.t other.

While spectral scanning is not preferable for EO applications, normally data are collected using pushbroom or whiskbroom approach for EO applications. In a pushbroom approach, data collects along track uses the line of detectors arranged perpendicular to the moving direction. In the push broom approach, all the pixels in a line are collected simultaneously. Whereas, in whiskbroom approach, data is collected across the track using a mirror which moves back and forth in order to collect the one-pixel data at a time.

Conceptual representation of hyperspectral imaging is shown in Fig. 3. In a given Figure, imaging spectrometer is attached to the flying platform and collecting data either along track or across track manner, where  $X$  and  $Y$  represent the spatial dimensions, while  $\lambda$  represents the spectral dimension of a hyperspectral data cube. In essence, hyperspectral data can be described as  $I(X, Y, \lambda)$  which can be viewed either as a spectral fingerprint  $I(\lambda)$  at each pixel  $(X, Y)$  or as a spatial distribution  $I(X, Y)$  at each wavelength  $(\lambda)$ . Spectral signature is generated at a specific pixel location by sampling the pixel values of all the spectral bands as shown in Fig. 3.

The major components of the hyperspectral imaging system are fore-optics, focussing optics, a spectral separation unit, illumination unit, translation stage, and detector system. Spaceborne and airborne platforms do not require illumination and translation units. The spectral separation unit may be grating, prism, an interferometer, electronic tunable filter (ETF), and linear variable filter (LVF)<sup>18</sup>. Each Spectral separation unit/device has its own advantages and disadvantages in terms of spectral resolution and range, compactness, throughput, etc.

In order to design and develop a system, simulation plays an important role in predicting and forecasting the performance of hyperspectral system prior to the development stage. Simulation provides an end to end simulation of the system to analyze and optimise the performance prior to development state. As a result, it is helpful to develop, validate, and implement the system. Sensor simulation also includes a spatial, spectral, and radiometric response of the system that are interpreted as key factors of image/data/spectral quality metrics as per the case<sup>19</sup>. SENSOR (Software Environment for the Simulation

of Optical Remote sensing systems)<sup>20</sup> is an end to end optical remote sensing simulation system that has been developed jointly by German Aerospace Centre (DLR) and University of Zurich to simulate imaging systems on airborne and spaceborne platforms. This simulator is divided into three modules: hardware, observed scene, and atmosphere. SENSOR simulator is closely related to an airborne hyperspectral sensor; Airborne Prism Experiment (APEX) by European Space Agency (ESA). Environmental Mapping and Analysis Program (EnMAP) simulator<sup>21</sup> has been developed to generate the hyperspectral and multispectral image by setting instrument and scene parameters prior to EnMAP mission to analyze the performance of the mission. EnMAP<sup>22</sup> is a German hyperspectral imager which works in the range of 420–2450 nm with a varying spectral sampling. CAMEO<sup>23</sup>, PICASSO<sup>24, 25</sup>, SG\_SIM<sup>26</sup> simulators have also been developed for end to end imaging chain analysis of the remote sensing system.

## 4 Platforms

Sensor systems should be placed over suitable observing platforms and lifted to pre-defined height. Platforms may be movable (airborne, spaceborne, aerial system or underwater vehicle) and stationary (field observation from the tripod) depend upon the requirements and constraints for observation. Generally, the spatial resolution of the imaging system starts decreasing as the height of the platform increases; however, the area of coverage also increases. Thus, a trade-off has to be carried out in between resolution and synoptic view to choose the proper platform height. Furthermore, stability and ability of the platform to support the sensor system need to be considered. Selection of the platform depends upon the application requirement and it may be satellite, aircraft, unmanned aerial system, underwater water vehicle or ground-based system. In this section we discuss the above mentioned moving platforms.

### 4.1 Airborne Platform

Aerial platform as the name suggests is that platform which remains in the air. It may be aircraft, balloon or helicopters which have been employed for aerial photography. Airborne remote sensing has been in practice since the past 30 years. They are generally used for local and/or limited region of interest. It may be done from low altitudes (1 km) to a few tens of kilometres depending on the capability of the aircraft and the integrated sensors. Initially, an analog camera has to be used with the airborne platform for aerial

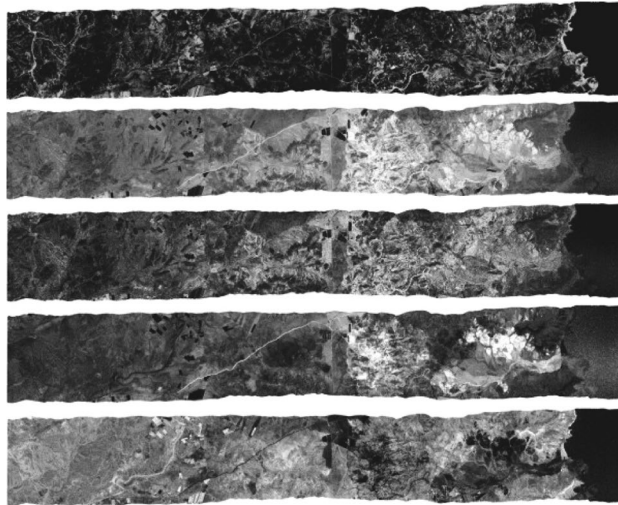


**Figure 4:** Mineral mapping of jarosite, kaolinite, illite, alunite, and chlorite<sup>27</sup>.

photography. Recent technological advancement enforces the airborne platform to be more sophisticated like digital camera along with GPS and image motion sensor to enhance the aerial photography and simultaneously provide extra information along with the image data. Currently, there are aircraft fitted with multiple numbers of sensors, capable of observing the whole range of electromagnetic spectrum in order to obtain the remote sensing data. Airborne hyperspectral

sensor, i.e., HyMAP data are shown in Fig. 4. It indicates mineral maps of jarosite, kaolinite, illite, alunite, and chlorite<sup>27</sup> in Rodalquilar.

The Main limitations of an airborne platform are the high cost for global coverage and regional coverage on a repetitive basis. Some of the major airborne hyperspectral sensors along with specifications of different countries have been given in Table 1.

**Table 1:** Some of the major airborne hyperspectral sensors along with specifications.

Instrument	Spectral range/bands	Manufacturer/producer	Launch date
AVIRIS-classic (Airborne visible infrared imaging spectrometer) <sup>28, 29</sup>	400–2500 nm/224	JPL, NASA	1986
Airborne imaging spectrometer (AIMS) <sup>30</sup>	454–888 nm/143	SAC-ISRO	1996
Airborne hyperspectral imager (AHySI) <sup>30</sup>	465–995 nm/512	SAC-ISRO	2007
AVIRIS-NG (Airborne visible infrared imaging spectrometer—Next Generation) <sup>31</sup>	380–2510 nm/	JPL, NASA	2012
HYDICE (Hyperspectral digital imagery collection experiment) <sup>32–34</sup>	400–2500 nm/210	U.S. Naval Research Laboratory	1995
CASI (Compact airborne spectrographic imager) <sup>35</sup>	430–870 nm/288	ITRES research	1988
HyMap (Hyperspectral Mapper) <sup>36, 37</sup>	450–2500 nm/100–200	Integrated Spectronics, Pty. Ltd.	
DAIS 7915 (Digital airborne imaging spectrometer) <sup>38</sup>	400–12300 nm/79	Geophysical Environmental Research	1996
ASAS (Advanced solid-state array spectroradiometer) <sup>39</sup>	450–880 nm/30	NASA Johnson Space Centre	
AAHIS (Advanced airborne hyperspectral imaging system) <sup>40</sup>	432–832 nm/288	SETS Technology Inc.	

**Table 2:** Some of the major spaceborne hyperspectral sensor missions along with specifications.

Instrument	Mission	Spectral range/bands	Launch date	Manufacturer/producer
Hyperion <sup>41</sup>	EO-1 (Earth Observing-1)	400–2500 nm/242	November, 2000	Northrop Grumman Space Technology, USA
CHRIS (Compact High Resolution Imaging Spectrometer) <sup>42, 43</sup>	PROBA (PProject for OnBoard Autonomy)	410–1050 nm/63	October, 2001	UK/ESA
HySI (Hyperspectral Imager) <sup>30, 44, 45</sup>	IMS-1(Indian Micro Satellite-1)	400–950 nm/64	April, 2008	ISRO, India
FTHSI (Fourier Transform Hyperspectral Imager) <sup>46</sup>	MightySat-II	475–1050 nm/146	July, 2000	Air Force Research Laboratory, USA
ARIES-1 (Australian Resource Information and Environmental Satellite) <sup>47</sup>	ARIES	400–1100nm and 2000–2500nm/64	2001	ARIES consortium of AUSPACE Limited
TG-1 HSI (TianGong-1 Hyperspectral Imager) <sup>48, 49</sup>	TianGong-1	400–1000 nm(10 nm) and 1000–2500 nm (23 nm) / 64(VNIR) and 64 (SWIR)		China Manned Space Engineering, China
HJ-1A HSI <sup>50</sup>	HJ-1 mission (Huan Jing-1)	450–950 nm/110–128	September, 2008	CAST, China
HICO (Hyperspectral Imager for the Coastal Ocean) <sup>51, 52</sup>		353–1081 nm/128	September, 2009	Naval Research Laboratory (NRL), USA

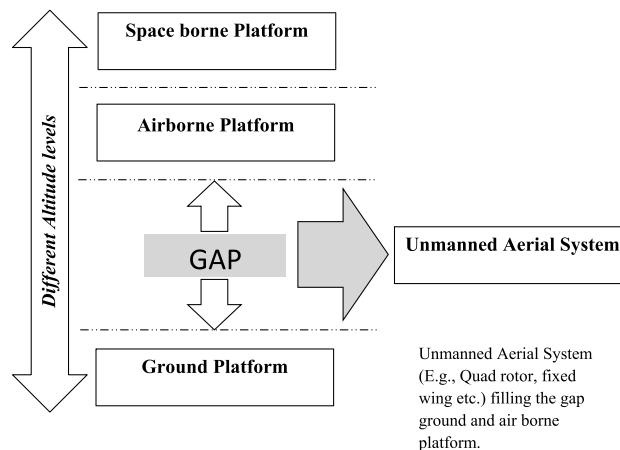


**Figure 5:** Relative importance of UAS hyperspectral remote sensing over Earth surface.

**4.2 Spaceborne Platform**

In spaceborne platforms, sensors are mounted on-board in the satellites and give a synoptic view of large areas. Spaceborne platforms (satellites) are placed in any of three orbits. Orbit may be LEO (Low Earth Orbit), MEO (Medium Earth Orbit), and GEO (Geostationary Earth Orbit). Each orbit has been used for specific application and has its own sensor designing as well as development criteria. In the spaceborne platform, the

imaging system design depends upon the type of orbit, its altitude w.r.t. earth, and instantaneous field of view (IFOV). The advantages of spaceborne platforms are wide-field of view (WFOV), coverage of large areas, and repetitive observations of the same area. On the contrary, it has some disadvantages like low spatial resolution (coarse mapping), performance degradation in the cloudy atmosphere, and onboard maintenance is not possible. Table 2 represents some of



the major spaceborne hyperspectral sensors of different organizations.

### 4.3 Unmanned Aerial System

UAS includes all vehicles with a fly in air capacity without an onboard person, able to control the flying vehicle. Hyperspectral imaging from spaceborne and airborne platforms is facing major challenges like the demand for high-resolution data, instant availability of data, and regionalized data. However, ground sensing platform faces difficulties in transportation and complexities in the generation of real-time ground maps besides the fewer possibilities of simultaneously collecting data from several plots. This suggests an alternative solution to address these issues, one of which is to use unmanned aerial system (UAS). Typically, UAS provides hyperspectral data with high spatial and temporal resolution which makes it vital for high-resolution EO applications. Conceptually, UAS bridges the gap between the airborne and ground-based platforms as shown in Fig. 5.

Cost and unavailability of high-resolution satellite imagery often limit the applications of hyperspectral imaging to EO. Consequently, UAS is cost-effective and better replacement of satellite and airborne for high-resolution imagery. In addition, UAS are the instantly accessible tool. Nowadays, UAS has been available in wide range from rotocopters to fixed wings<sup>53</sup>. UAS has been divided mainly into four categories, i.e., parachutes, blimps, rotocopters, and fixed wing systems. Each category has its own conditions and limitations. Under no-wind conditions, parachutes can be flown but not in windy

conditions. Moreover, they are relatively slow and take less flight time. Generally, blimps are used for advertising and can be used for aerial photography. However, they move slowly from one place to another due to the large surface area. Most widely used UAS are rotocopters and fixed wings. Rotocopters have a number of advantages like flying horizontally and vertically, hovering at a given location. However, limitations are low speed and flight time as compared to fixed wings. On the contrary, fixed wings have high speed and flight time. However, they do not have hovering capability.

UAS has been capable to take images at high resolution for monitoring and measuring the environmental conditions on a regional basis. Advancement of technology led to the availability of lightweight hyperspectral sensors commercially. This makes possible to integrate the lightweight hyperspectral sensor with UAS. It is one of the cost-effective and preferable solutions in place of spaceborne and airborne platforms to collect high-resolution data on requirement basis. The number of sensors can be integrated with the UAS platforms depending on payload lift capabilities, type of data requirement including hyperspectral sensor<sup>54, 55</sup>, LiDAR (Light Detection and Ranging) sensor<sup>56</sup>, multispectral sensor<sup>57, 58</sup>, GPS, thermal camera<sup>59, 60</sup>, digital camera<sup>61</sup>, etc. This type of system has been used extensively in ge-resources applications and precision agriculture<sup>53, 62–64</sup>.

The successful implementation of UAS for EO applications depends on two main factors<sup>62</sup>. The first is UAS characteristics such as safety, stability, control, endurance, positioning, autonomy, and

**Table 3:** Some of the major UAS for Earth observation applications.

Type	Manufacturer/model	Weight/payload (kg)	Altitude (m)	Flying speed (km/h)
Fixed-wing	Precisionhawk/LANCASTER 5	2.4	2500 (max.)	79
	Trimble/UX5	2.5	75–750	80
	AeroVironment/Puma AE RQ-20B	6.3	150	47–83
helicopter	High eye/HEF 30	< 25/5	1800	130
	Aeroscout GmbH/Scout B1-100	50/18	5000	
hexacopter	Aibotix/Aibot X6	3.4	3000	40
	Vespadrones/XYRIS 6	4.2/2.2		80
	dji/MATRICE 600 PRO	10/5.5	5000	65
Octocopter	Ascending/Intel Falcon 8+	1.2	4000	
Dodecarotor	Altigator/HYDRA-12	/12		
Quadrocopter	microdrones/MD4-3000	6/3	4000	72

Specifications are taken from the manufacturer's websites

**Table 4:** Some of the major hyperspectral cameras for UAS and ground sensing platform.

Manufacturer	Model	Spectral range/bands	Weight (kg)	Technology
Resonon	Pika L	400–1000 nm /281	0.6	Pushbroom
	Pika NIR	900–1700 nm /164	2.7	Pushbroom
	Pika NUV	350–800 nm/196	2.1	
	Pika XC2	400–1000 nm/447	2.2	
Surface optics	SOC710-GX	400–1000 nm /120	1.25	
Bayspec	OCI-UAV-1000	600–1000 nm /100	0.180	Pushbroom
HySpex	HySpex Mjolnir-1024	400–1000 nm /200	4.0	
Headwall	Nano-Hyperspec	400–1000 nm /270	0.52	
Specim	AISAKESTREL 10	400–1000 nm /	2.1	Pushbroom
	AISAKESTREL 16	600–1640 nm /	2.3	Pushbroom
	OWL	8000-12000 nm /84	3.5	Pushbroom
	sCMOS-50-V8E	400–1000 nm /	2.0	Pushbroom
Ximea	MQ022HG-IM-LS100-NIR	630–970 nm/100+	0.032	Linescan
	MQ022HG-IM-LS150-VISNIR	470–900 nm/150+	0.032	Linescan
	MQ022HG-IM-SM4X4-VIS	470–630 nm/16	0.032	Snapshot Mosaic
	MQ022HG-IM-SM5X5-NIR	600–975 nm/25	0.032	Snapshot Mosaic
Itres	micro CASI 1920	400–1000 nm/288	< 1.5	Pushbroom
	micro SASI 384	1000–2500 nm/200	2.0	Pushbroom
Corning	microHSI 410 SHARK	400–1000 nm/	0.68	
Cubert GmbH	S 185 FirefLEYE SE	450–950 nm/125	0.49	Snapshot
Rikola	VIS-VNIR Snapshot	400–1000 nm/380	0.720	Snapshot

Specifications are taken from the manufacturer's websites

sensor mount. The second is sensor characteristics such as resolution, weight, and field of view. There is a need to take care above aspects in order to utilize the full potential for EO applications. Irrespective of this, an improvement over hyperspectral data processing algorithms is required for automatic feature extraction, geo-referencing, blur reduction, and distortion correction. UAS provides an opportunity for high throughput for EO applications. We expect the usage of UAS-based technology will grow exponentially in upcoming few years. Tables 3 and 4 represent some of the majorly available UAS platforms and cameras for Earth observation applications.

#### 4.4 Ground-Based Platform

For ground-based hyperspectral sensing, a mobile or static platform has also been used for data collection. Data are collected at ground level by fixing a hyperspectral imaging system on to the moving or static platform. Portable handheld spectro-radiometer provides the spectral information of the material under test used

for calibration and analysis process of collected hyperspectral data<sup>65–67</sup>. Such devices have been frequently used in mining<sup>68</sup> and agricultural<sup>69</sup> applications to determine the spectral behavior of the material under study. The static platform offers better observation capabilities and temporal resolution. It has been used in numerous applications like toxic industrial chemicals and gases detection<sup>70</sup>, volcanology, natural gas, combustion analysis, and camouflage<sup>71</sup>. Generally, spectro-radiometer is not used with a mobile vehicle because of the fact that the data captured by it is localized and limited analysis. Nowadays, a mobile hyperspectral vehicle for ground sensing has been gaining popularity and usability<sup>72, 73</sup>. A mobile vehicle is composed of imaging, synchronization, and navigation sensors in which it includes a hyperspectral camera, digital camera, navigation sensors, and GPS for geo-referencing, is being studied and tested for field applications to improve the data density in spatial as well as temporal scales. Table 4 represents some of the



**Table 5:** Some of the major underwater vehicles.

Manufacturer	Model	Operating depth	Weight (Kg)
Hydroid	Remus 100	100 m	
	Remus 600	600/500m	
	Remus 6000	6000 m	
Kongsberg	Seaglider	50 to 1000 m	
	Hugin	3000/4500/6000 m	
	Munin	600/1500 m	
Teledyne Marine	Gavia Scientific AUV	500/1000 m	
	Gavia Offshore Surveyor	500/1000 m	
	Gavia Defence AUV	500/1000 m	
Bluefin	Bluefin-21	4500 m	
	Bluefin Sand-Shark	200 m	
	HAUV	30/60 m	
Ageotec-Lighthouse	ROV SIRIO	300 m	40
	ROV LYRA	300 m	80
	ROV PER-SEO	300 m	80
	ROV PER-SEO GTV	1500 m	160
	ROV PEGASO	1500 m	400
Fugro	ECHO SURVEYOR II	3000 m	1450
	ECHO SURVEYOR IV	3000 m	1860
	ECHO SURVEYOR VII	4500 m	1700
	seaeye falcon	300 m	60
	Seaeye TIGER	600/1000 msw	150
	seaeye lynx	1500 msw	200
	SEAEYE COUGAR-XT	2000 m	409
	SEAEYE PANTHER PLUS	1000 msw	500
	SEAEYE PANTHER XT	1500 msw	500

Table 5: continued

Manufacturer	Model	Operating depth	Weight (Kg)
Forum Energy	XLX-C	3000 (4000) msw	3600–4100 kg
	XLX 200HP	3000 (4000) m	5500 (5662) kg
	Mojave	300 m	85
	Mohican	2000 m	340
	Mohawk	2000 m	165
	Comanche	3000 m	1130
	Super Mohawk	3000 m	395
Subsea Tech	Observer 4.0	150 m	6.4
	Guardian 3.0	150 m	4.5
AC-CESS	AC-ROV 100	100 msw	3
	AC-ROV 3000	100 m	3
Blue Robotics	BlueROV2	100 m	10–11
Dwitek	Investigator 90	500 m	132
Mariner Underwater	IPPODA-MUS	750 msw	75

Specifications are taken from the manufacturer's websites

major hyperspectral cameras of public and private organizations.

#### 4.5 Underwater Vehicle

The Knowledge of the underwater environment is limited as compared to the over surface environment of the Earth. Over the past few decades, remote sensing from satellites and aircrafts has shown significant improvement in a number of applications such as agriculture<sup>74, 75</sup>, geology<sup>27, 76</sup>, forestry<sup>77, 78</sup>, and archeology<sup>79, 80</sup>. However, many of the over surface techniques do not work in the underwater environment. The underwater environment is complex and dynamic, executes large unevenness in bio-geo-chemical composition over space and time. There is a requirement to collect seafloor (underwater) data in order to perform continuous monitoring, management, and mapping of the underwater environment. Conventional methods like in situ diver surveys, video towed from boat, etc. are used for the underwater survey. However, they are limited in order to provide high-quality maps of the

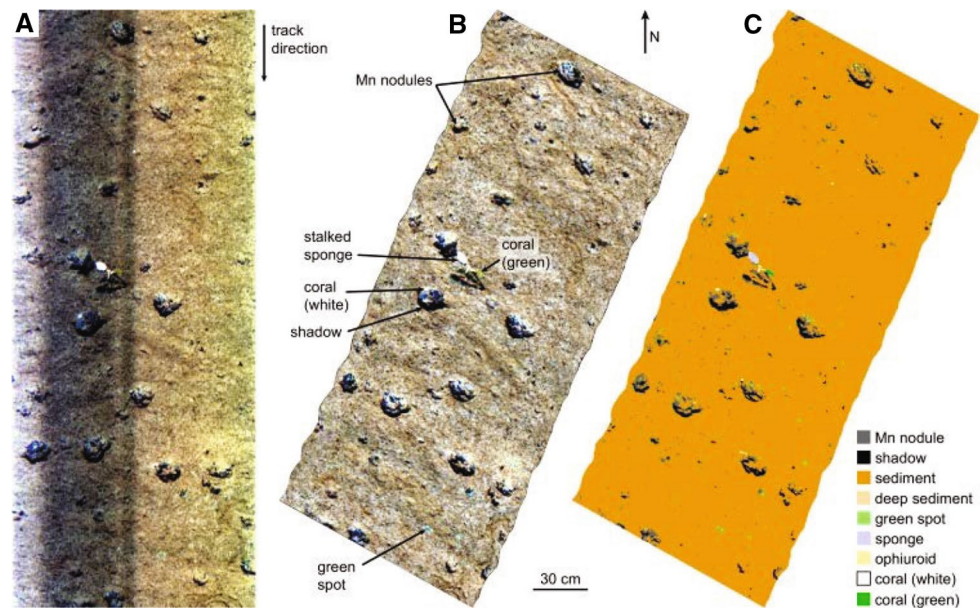


**Figure 6:** **a** Radiance data in pseudo-RGB (R: 645 nm, G: 571 nm, B: 473 nm), **b** geocorrected pseudo-reflectance data in pseud-RGB, and **c** support vector machine classification image based on the data given in (**b**) section. Dumke et al.(2018)<sup>83</sup>.

**Table 6:** Some of the major underwater hyperspectral cameras.

Model	Manufacturer	Spectral range/bands	Technology
Underwater hyperspectral imager (UHI)	Ecotone		Pushbroom
WaterCam	SphereOptics	450–950 nm/138	Snapshot
S 685-FirefLEYE UW	Cubert GmbH	450–950 nm/125	Non-scanning

Specifications are taken from the manufacturer's websites

underwater features. In such a case, an underwater vehicle can be used to collect data for monitoring and mapping of the seafloor bed. During the last decade, a semi-autonomous/autonomous vehicle has been advancing from experimental setup to commercial system for the underwater environment. Underwater vehicle has been used for marine coastal monitoring<sup>81</sup>, mapping, and management to determine biological abundance, diversity and behavior, marine traffic, and construction work<sup>82</sup> to make sustainable decisions for the environment.

With an underwater vehicle, hyperspectral imaging is used to obtain qualitative and quantitative information of the material of interest. This technique provides an optical fingerprint of the minerals, seagrass, coral reef from visible to Infra-Red (IR) range to identify and map the target of interest. Passive hyperspectral imaging is possible in optically shallow areas. Such technique is

used to map seagrass<sup>83</sup>, near-shore habitats<sup>84</sup> and kelp<sup>85</sup>. Most of the sea areas are optically deep and cannot be imaged using passive hyperspectral imaging technique. In such scenario, passive imaging technique does not work for optically deep areas, requires a light source for illumination. AN artificial light source has been used to utilize the full potential of underwater hyperspectral imaging. Hyperspectral imager positioned into the Remotely Operated Vehicles (ROV)<sup>86</sup> and Autonomous Underwater Vehicles (AUV) to collect the seafloor reflectance data. In order to overcome the passive imaging effects, illumination unit is used to measure the benthic reflectance at high spectral and spatial resolution. Light source should be designed specifically to illuminate the object of interest evenly.

Hyperspectral imaging is one of the potential techniques for mapping and monitoring of the underwater environment. Limited literature

is available for the hyperspectral sensing underwater vehicle as compared with other platforms for surface observation. ROV and AUV may be used for underwater surface inspection. There are numbers of underwater vehicles commercially available. Each vehicle has its own operating depth range, endurance, speed, the payload carrying capability, sensor integration interfaces, battery working time and so on. Some of the available underwater vehicles are integrated with sensors and others provide options to interface sensors. Therefore, Usability, application domains, type of data requirement, etc. may vary in each case. Some of the underwater vehicles list which may be used with a hyperspectral sensor and/or with different sensors (LiDAR, SONAR, etc.) for underwater monitoring are given in Table 5.

Pushbroom sensor design<sup>87</sup> may be used to conduct high-quality underwater hyperspectral imaging, where the scan line is perpendicular to the direction of imaging. Underwater hyperspectral imaging is used for mapping, monitoring, and identification of deepwater species, habitats, marine mining applications, and undersea pipeline inspection. Furthermore, underwater hyperspectral data are used as an input to improve the autonomy of underwater vehicle for planning and navigation. Johnsen et al.<sup>86</sup> positioned underwater hyperspectral imaging into ROVs for automated mapping, monitoring, and identification of underwater bio-geo-chemical materials. Similarly, Odegard et al.<sup>88</sup> surveyed underwater archaeological sites by unmanned platforms integrated with acoustic sensors and optical sensors. The purpose of this study was to demonstrate the advanced underwater technology and marine robotics for surveying. In<sup>89</sup>, authors presented the first hyperspectral data from the deep sea floor and checked the potential of the underwater hyperspectral imager (UHI) for seafloor exploration. In this, authors compared two supervised classification methods, i.e., spectral angle mapper and support vector machine for detection and mapping of minerals in the deep sea. Data are collected in approximately 4200 m water depth by pushbroom UHI (378–805 nm) developed by Ecotone. The KIEL6000 ROV(GEOMAR) is used as a UHI platform for data collection. Herein, underwater hyperspectral Data processing consist of three steps. They are radiance processing, (pseudo-)reflectance processing, and geocorrection via photomosaic-based navigation data. Underwater hyperspectral data have been shown in Fig. 6a, b and c. Calibration of raw data to radiance by radiometric

calibration has been shown in Fig. 6(A). Geocorrected pseudo-reflectance data have been shown in Fig. 6(B) and classified image by support vector machine has been shown in Fig. 6(C). Authors concluded that the underwater hyperspectral imaging has a potential to survey from shallow coastal water to deep sea for mapping and classification.

Other sensors like LiDAR<sup>90</sup>, side scan sonar, synthetic aperture sonar, and stereo cameras<sup>88, 91</sup> have also been used in an unmanned underwater platform for surveying and inspection application. Some of the available underwater hyperspectral cameras have been given in Table 6.

## 5 Conclusion

Hyperspectral imaging has been gaining popularity from space imaging to machine vision applications. We need to know the sensing platforms and instruments in order to acquire hyperspectral data effectively for different applications. In this article, we have briefly discussed different sensing movable platforms for EO applications. Additionally, some of the major hyperspectral instruments for different sensing platforms developed by several public and private organizations are presented. As a conclusion, It is anticipated more instruments with better specifications for different sensing platforms will continue to expand for EO applications.

Received: 29 November 2017 Accepted: 23 April 2018  
Published online: 9 May 2018

## References

1. Liu D, Zeng XA, Sun DW (2015) Recent developments and applications of hyperspectral imaging for quality evaluation of agricultural products: a review. *Crit Rev Food Sci Nutr* 55(12):1744–1757
2. He HJ, Sun DW (2015) Hyperspectral imaging technology for rapid detection of various microbial contaminants in agricultural and food products. *Trends Food Sci Technol* 46(1):99–109
3. Huang H, Liu L, Ngadi MO (2014) Recent developments in hyperspectral imaging for assessment of food quality and safety. *Sensors* 14(4):7248–7276
4. Wang NN, Sun DW, Yang YC, Pu H, Zhu Z (2016) Recent advances in the application of hyperspectral imaging for evaluating fruit quality. *Food Anal Methods* 9(1):178–191
5. Calin MA, Parasca SV, Savastru D, Manea D (2014) Hyperspectral imaging in the medical field: present and future. *Appl Spectrosc Rev* 49(6):435–447
6. Lu G, Fei B (2014) Medical hyperspectral imaging: a review. *J Biomed Opt* 19(1):010901

7. Randolph K, Wilson J, Tedesco L, Li L, Pascual DL, Soyeux E (2008) Hyperspectral remote sensing of cyanobacteria in turbid productive water using optically active pigments, chlorophyll a and phycocyanin. *Remote Sens Environ* 112(11):4009–4019
8. Brando VE, Dekker AG (2003) Satellite hyperspectral remote sensing for estimating estuarine and coastal water quality. *IEEE Trans Geosci Remote Sens* 41(6):1378–1387
9. Thenkabail PS, Lyon JG, Huete A (2016) Hyperspectral remote sensing of vegetation. CRC Press, Boca Raton
10. Kozoderov V, Kondranin T, Dmitriev E, Kamentsev V (2014) A system for processing hyperspectral imagery: application to detecting forest species. *Int J Remote Sens* 35(15):5926–5945
11. Jing C, Bokun Y, Runsheng W, Feng T, Yingjun Z, Dechang L, Suming Y, Wei S (2014) Regional-scale mineral mapping using aster vnir/swir data and validation of reflectance and mineral map products using airborne hyperspectral casi/sasi data. *Int J Appl Earth Obs Geoinf* 33:127–141
12. Puckrin E, Turcotte CS, Gagnon MA, Bastedo J, Farley V, Chamberland M (2012) Airborne infrared hyperspectral imager for intelligence, surveillance, and reconnaissance applications. In: *SPIE Defense, Security, and Sensing*, p. 836,004. International Society for Optics and Photonics
13. Cucci C, Delaney JK, Picollo M (2016) Reflectance hyperspectral imaging for investigation of works of art: old master paintings and illuminated manuscripts. *Acc Chem Res* 49(10):2070–2079
14. Fischer C, Kakoulli I (2006) Multispectral and hyperspectral imaging technologies in conservation: current research and potential applications. *Stud Conserv* 51(sup1):3–16
15. Hege EK, O'Connell D, Johnson W, Basty S, Dereniak EL (2004) Hyperspectral imaging for astronomy and space surveillance. In: *Optical Science and Technology, SPIE's 48th Annual Meeting*, pp. 380–391. International Society for Optics and Photonics
16. Bradley BA (2014) Remote detection of invasive plants: a review of spectral, textural and phenological approaches. *Biol Invasions* 16(7):1411–1425
17. Shaw GA, Burke HHK (2003) Spectral imaging for remote sensing. *Linc Lab J* 14(1):3–28
18. Kiran Kumar AS, Roy Chowdhury AR, Banerjee A, Dave AB, Sharma BN, Shah KJ, Murali KR, Mehta S, Joshi SR, Sarkar SS (2009) Hyper Spectral Imager for lunar mineral mapping in visible and near infrared band. *Curr Sci* 96(4):496–499
19. Kerekes JP, Cisz AP, Simmons RE (2005) A comparative evaluation of spectral quality metrics for hyperspectral imagery. In: *Defense and security. International Society for optics and photonics*. pp. 469–480. <https://doi.org/10.1117/12.605916>
20. Börner A, Wiest L, Keller P, Reulke R, Richter R, Schaepman M, Schlöpfer D (2001) Sensor: a tool for the simulation of hyperspectral remote sensing systems. *ISPRS J Photogramm Remote Sens* 55(5):299–312. [https://doi.org/10.1016/S0924-2716\(01\)00022-3](https://doi.org/10.1016/S0924-2716(01)00022-3)
21. Guanter L, Segl K, Kaufmann H (2009) Simulation of optical remote-sensing scenes with application to the enmap hyperspectral mission. *Geosci Remote Sens IEEE Trans* 47(7):2340–2351. <https://doi.org/10.1109/TGRS.2008.2011616>
22. Stuffer T, Kaufmann C, Hofer S, Förster K, Schreier G, Mueller A, Eckardt A, Bach H, Penne B, Benz U et al (2007) The enmap hyperspectral imager: an advanced optical payload for future applications in earth observation programmes. *Acta Astronaut* 61(1):115–120. <https://doi.org/10.1016/j.actaastro.2007.01.033>
23. Moorhead IR, Gilmore MA, Houlbrook AW, Oxford DE, Filbee D, Stroud C, Hutchings G, Kirk A (2001) Cameo-sim: a physics-based broadband scene simulation tool for assessment of camouflage, concealment, and deception methodologies. *Opt Eng* 40(9):1896–1905. <https://doi.org/10.1117/1.1390298>
24. Cota SA, Bell JT, Boucher RH, Dutton TE, Florio CJ, Franz GA, Grycewicz TJ, Kalman LS, Keller RA, Lomheim TS et al (2010) Picasso: an end-to-end image simulation tool for space and airborne imaging systems. *J Appl Remote Sens* 4(1):043535. <https://doi.org/10.1117/1.3457476>
25. Cota SA, Lomheim TS, Florio CJ, Harbold JM, Muto BM, Schoolar RB, Wintz DT, Keller RA (2011) Picasso: an end-to-end image simulation tool for space and airborne imaging systems ii. Extension to the thermal infrared: equations and methods. In: *SPIE optical engineering+ applications, International society for optics and photonics*, pp. 81,580G. <https://doi.org/10.1117/12.892808>
26. Coppo P, Chiarantini L, Alparone L (2013) End-to-end image simulator for optical imaging systems: equations and simulation examples. *Adv Opt Technol*. DOI:10.1155/2013/295950
27. Van der Meer FD, Van der Werff HM, van Ruitenbeek FJ, Hecker CA, Bakker WH, Noomen MF, van der Meijde M, Carranza EJM, de Smeth JB, Woldai T (2012) Multi- and hyperspectral geologic remote sensing: a review. *Int J Appl Earth Obs Geoinf* 14(1):112–128
28. Vane G, Green RO, Chrien TG, Enmark HT, Hansen EG, Porter WM (1993) The airborne visible/infrared imaging spectrometer (aviris). *Remote Sens Environ* 44(2–3):127–143. [https://doi.org/10.1016/0034-4257\(93\)90012-M](https://doi.org/10.1016/0034-4257(93)90012-M)
29. Green RO, Eastwood ML, Sarture CM, Chrien TG, Aronsson M, Chippendale BJ, Faust JA, Pavri BE, Chovit CJ, Solis M et al (1998) Imaging spectroscopy and the airborne visible/infrared imaging spectrometer (aviris). *Remote Sens Environ* 65(3):227–248. [https://doi.org/10.1016/S0034-4257\(98\)00064-9](https://doi.org/10.1016/S0034-4257(98)00064-9)
30. Kumar KA, Thapa N, Kuriakose SA (2015) Advances in spaceborne hyperspectral imaging systems. *Curr Sci* 108(5):826
31. Bue BD, Thompson DR, Eastwood M, Green RO, Gao BC, Keymeulen D, Sarture CM, Mazer AS, Luong HH (2015)



- Real-time atmospheric correction of aviris-ng imagery. *IEEE Trans Geosci Remote Sens* 53(12):6419–6428
32. Basedow RW, Carmer DC, Anderson ME (1995) Hydice system: implementation and performance. In: SPIE's 1995 symposium on OE/aerospace sensing and dual use photonics, International Society for Optics and Photonics, pp. 258–267. <https://doi.org/10.1117/12.210881>
  33. Resmini R, Kappus M, Aldrich W, Harsanyi J, Anderson M (1997) Mineral mapping with hyperspectral digital imagery collection experiment (hydice) sensor data at cuprite, nevada, usa. *Int J Remote Sens* 18(7):1553–1570
  34. Nischan ML, Kerekes JP, Baum JE, Basedow RW (1999) Analysis of hydice noise characteristics and their impact on subpixel object detection. In: SPIE's International Symposium on optical science, engineering, and instrumentation, International Society for Optics and Photonics, pp. 112–123
  35. Babey SK, Anger CD (1993) Compact airborne spectrographic imager (casi): a progress review. In: Optical Engineering and Photonics in Aerospace Sensing, International society for optics and photonics, pp. 152–163. <https://doi.org/10.1117/12.157052>
  36. Cocks T, Jenssen R, Stewart A, Wilson I, Shields T (1998) The hymaptm airborne hyperspectral sensor: The system, calibration and performance. European Assoc Remote Sensing Laboratories, Versailles
  37. Kruse F, Boardman J, Lefkoff A, Young J, Kierein-Young K, Cocks T, Jensen R, Cocks P (2000) Hymap: an australian hyperspectral sensor solving global problems-results from USA hymap data acquisitions. In: Proceeding of the 10th Australasian Remote Sensing and Photogrammetry Conference, pp. 18–23
  38. Chang SH, Westfield MJ, Lehmann F, Oertel D, Richter R (1993) 79-channel airborne imaging spectrometer. In: Optical engineering and photonics in aerospace sensing, International Society for Optics and Photonics, pp. 164–172. <https://doi.org/10.1117/12.157053>
  39. Huegel FG (1987) Advanced solidstate array spectroradiometer: sensor and calibration improvements. In: 31st Annual technical symposium, International Society for Optics and Photonics, pp. 12–15. <https://doi.org/10.1117/12.942278>
  40. Voelker MA, Resmini RG, Mooradian GC, McCord TB, Warren CP, Fene MW, Coyle CC, Anderson R (1995) Advanced airborne hyperspectral imaging system (aahis): an imaging spectrometer for maritime applications. In: SPIE's 1995 Symposium on OE/Aerospace sensing and dual use photonics, International Society for Optics and Photonics, pp. 357–367. <https://doi.org/10.1117/12.210891>
  41. Pearlman JS, Barry PS, Segal CC, Shepanski J, Beiso D, Carman SL (2003) Hyperion, a space-based imaging spectrometer. *Geosci Remote Sens IEEE Trans* 41(6):1160–1173. <https://doi.org/10.1109/TGRS.2003.815018>
  42. Van Mol B, Ruddick K (2004) The compact high resolution imaging spectrometer (chris): the future of hyperspectral satellite sensors. imagery of oostende coastal and inland waters. In: Proceedings of the Airborne Imaging Spectroscopy workshop, Brugge
  43. Cutter MA, Lobb DR, Cockshott RA (2000) Compact high resolution imaging spectrometer (chris). *Acta Astronaut* 46(2):263–268. [https://doi.org/10.1016/S0094-5765\(99\)00207-6](https://doi.org/10.1016/S0094-5765(99)00207-6)
  44. Kumar A, Saha A, Dadhwal V (2010) Some issues related with sub-pixel classification using hysi data from ims-1 satellite. *J Indian Soc Remote Sens* 38(2):203–210. <https://doi.org/10.1007/s12524-010-0027-5>
  45. Kuriakose SA, Subrahmanyam D, Sarkar S, Patel V, Mathur N (2006) Design and development of the multispectral payload for twosat mission. In: Asia-Pacific remote sensing symposium, International society for optics and photonics, pp. 640,516. <https://doi.org/10.1117/12.693863>
  46. Yarbrough S, Caudill TR, Kouba ET, Osweiler V, Arnold J, Quarles R, Russell J, Otten III LJ, Jones BA, Edwards A et al (2002) Mightysat ii. 1 hyperspectral imager: summary of on-orbit performance. In: International symposium on optical science and technology, International Society for Optics and Photonics, pp. 186–197. <https://doi.org/10.1117/12.453339>
  47. Roberts E, Huntington J, Denize R (1997) The australian resource information and environment satellite (aries), phase a study
  48. Gu Y, Gao M, Zhao G, Liu Y, Jin Z (2014) Science researches of Chinese manned space flight. *Chin J Space Sci* 34(5):518–524
  49. Li X, Wu T, Liu K, Li Y, Zhang L (2016) Evaluation of the Chinese fine spatial resolution hyperspectral satellite tiangong-1 in urban land-cover classification. *Remote Sens* 8(5):438
  50. Zhang B, Chen Z, Li J, Gao L (2009) Image quality evaluation on chinese first earth observation hyperspectral satellite. In: Geoscience and remote sensing symposium, 2009 IEEE International, IGARSS 2009, vol. 1, pp. 1–188. <https://doi.org/10.1109/IGARSS.2009.5416885>
  51. Lucke RL, Corson M, McGlothlin NR, Butcher SD, Wood DL, Korwan DR, Li RR, Snyder WA, Davis CO, Chen DT (2011) Hyperspectral imager for the coastal ocean: instrument description and first images. *Appl Opt* 50(11):1501–1516. <https://doi.org/10.1364/AO.50.001501>
  52. Corson MR, Korwan DR, Lucke RL, Snyder WA, Davis CO (2008) The hyperspectral imager for the coastal ocean (hico) on the international space station. In: Geoscience and remote sensing symposium, 2008. IGARSS 2008. IEEE International, vol. 4, pp. IV–101. IEEE. <https://doi.org/10.1109/IGARSS.2008.4779666>
  53. Zhang C, Kovacs JM (2012) The application of small unmanned aerial systems for precision agriculture:

- a review. *Precis Agric* 13(6):693–712. <https://doi.org/10.1007/s11119-012-9274-5>
54. Suomalainen J, Anders N, Iqbal S, Roerink G, Franke J, Wenting P, Hünninger D, Bartholomeus H, Becker R, Kooistra L (2014) A lightweight hyperspectral mapping system and photogrammetric processing chain for unmanned aerial vehicles. *Remote Sens* 6(11):11013–11030
  55. Zarco-Tejada PJ, González-Dugo V, Berni JA (2012) Fluorescence, temperature and narrow-band indices acquired from a uav platform for water stress detection using a micro-hyperspectral imager and a thermal camera. *Remote Sens Environ* 117:322–337
  56. Wallace L, Lucieer A, Watson C, Turner D (2012) Development of a UAV-lidar system with application to forest inventory. *Remote Sens* 4(6):1519–1543
  57. Berni JA, Zarco-Tejada PJ, Suárez L, Fereres E (2009) Thermal and narrowband multispectral remote sensing for vegetation monitoring from an unmanned aerial vehicle. *IEEE Trans Geosci Remote Sens* 47(3):722–738
  58. Turner D, Lucieer A, Watson C (2011) Development of an unmanned aerial vehicle (UAV) for hyper resolution vineyard mapping based on visible, multispectral, and thermal imagery. In: *Proceedings of 34th International symposium on remote sensing of environment*, p. 4
  59. Baluja J, Diago MP, Balda P, Zorer R, Meggio F, Morales F, Tardaguila J (2012) Assessment of vineyard water status variability by thermal and multispectral imagery using an unmanned aerial vehicle (UAV). *Irrig Sci* 30(6):511–522
  60. Gonzalez-Dugo V, Zarco-Tejada P, Nicolás E, Nortés PA, Alarcón JJ, Intrigliolo DS, Fereres E (2013) Using high resolution uav thermal imagery to assess the variability in the water status of five fruit tree species within a commercial orchard. *Precis Agric* 14(6):660–678
  61. Ahmad A, Samad AM (2010) Aerial mapping using high resolution digital camera and unmanned aerial vehicle for geographical information system. In: *Signal Processing and Its Applications (CSPA), 2010 6th International Colloquium on*, pp. 1–6. IEEE
  62. Sankaran S, Khot LR, Espinoza CZ, Jarolmasjed S, Sathuvalli VR, Vandemark GJ, Miklas PN, Carter AH, Pumphrey MO, Knowles NR et al (2015) Low-altitude, high-resolution aerial imaging systems for row and field crop phenotyping: a review. *Eur J Agronomy* 70:112–123. <https://doi.org/10.1016/j.eja.2015.07.004>
  63. Swain KC, Jayasuriya HP, Salokhe VM (2007) Suitability of low-altitude remote sensing images for estimating nitrogen treatment variations in rice cropping for precision agriculture adoption. *J Appl Remote Sens* 1(1):013547. <https://doi.org/10.1117/1.2824287>
  64. Primicerio J, Di Gennaro SF, Fiorillo E, Genesisio L, Lugato E, Matese A, Vaccari FP (2012) A flexible unmanned aerial vehicle for precision agriculture. *Precis Agric* 13(4):517–523. <https://doi.org/10.1007/s11119-012-9257-6>
  65. Hadley BC, Garcia-Quijano M, Jensen JR, Tullis JA (2005) Empirical versus model-based atmospheric correction of digital airborne imaging spectrometer hyperspectral data. *Geocarto Int* 20(4):21–28. <https://doi.org/10.1080/10106040508542360>
  66. Glenn NE, Mundt JT, Weber KT, Prather TS, Lass LW, Pettingill J (2005) Hyperspectral data processing for repeat detection of small infestations of leafy spurge. *Remote Sens Environ* 95(3):399–412. <https://doi.org/10.1016/j.rse.2005.01.003>
  67. Crouvi O, Ben-Dor E, Beyth M, Avigad D, Amit R (2006) Quantitative mapping of arid alluvial fan surfaces using field spectrometer and hyperspectral remote sensing. *Remote Sens Environ* 104(1):103–117. <https://doi.org/10.1016/j.rse.2006.05.004>
  68. Gladwell D, Lett R, Lawrence P (1983) Application of reflectance spectrometry to mineral exploration using portable radiometers. *Econ Geol* 78(4):699–710. <https://doi.org/10.2113/gsecongeo.78.4.699>
  69. Shibayama M, Takahashi W, Morinaga S, Akiyama T (1993) Canopy water deficit detection in paddy rice using a high resolution field spectroradiometer. *Remote Sens Environ* 45(2):117–126. [https://doi.org/10.1016/0034-4257\(93\)90036-W](https://doi.org/10.1016/0034-4257(93)90036-W)
  70. Fortin G, Thériault JM, Lacasse P (2013) LWIR polarization sensing: investigation of liquids and solids with moddifs. In: *SPIE optical engineering+ applications, International society for optics and photonics*, pp. 88,730H
  71. Montembeault Y, Lagueux P, Farley V, Villemaire A, Gross KC (2010) Hyper-cam: hyperspectral ir imaging applications in defence innovative research. In: *Hyperspectral image and signal processing: evolution in remote sensing (WHISPERS), 2010 2nd Workshop on*, pp. 1–4. IEEE
  72. Reyniers M, Vrindts E (2006) Measuring wheat nitrogen status from space and ground-based platform. *Int J Remote Sens* 27(3):549–567. <https://doi.org/10.1080/01431160500117907>
  73. Abd-Elrahman A, Pande-Chhetri R, Vallad G (2011) Design and development of a multi-purpose low-cost hyperspectral imaging system. *Remote Sens* 3(3):570–586. <https://doi.org/10.3390/rs3030570>
  74. Atzberger C (2013) Advances in remote sensing of agriculture: Context description, existing operational monitoring systems and major information needs. *Remote Sens* 5(2):949–981
  75. Lelong CC, Pinet PC, Poilvé H (1998) Hyperspectral imaging and stress mapping in agriculture: a case study on wheat in beauce (france). *Remote Sens Environ* 66(2):179–191
  76. Cloutis E (1996) Review article hyperspectral geological remote sensing: evaluation of analytical techniques. *Int J Remote Sens* 17(12):2215–2242
  77. Holmgren P, Thuresson T (1998) Satellite remote sensing for forestry planning: a review. *Scand J For Res* 13(1–4):90–110



78. Coppin PR, Bauer ME (1996) Digital change detection in forest ecosystems with remote sensing imagery. *Remote Sens Rev* 13(3–4):207–234
79. Kucukkaya AG (2004) Photogrammetry and remote sensing in archeology. *J Quant Spectrosc Radiat Transf* 88(1):83–88
80. Saturno W, Sever TL, Irwin DE, Howell BF, Garrison TG (2006) Putting us on the map: remote sensing investigation of the ancient maya landscape. In: *Remote sensing in archaeology*, Springer, pp. 137–160
81. Barrett N, Seiler J, Anderson T, Williams S, Nichol S, Hill SN (2010) Autonomous underwater vehicle (AUV) for mapping marine biodiversity in coastal and shelf waters: implications for marine management. In: *OCEANS 2010 IEEE-Sydney*, IEEE, pp. 1–6
82. Ludvigsen M, Thorsnes T, Hansen RE, Johnsen G, Lågstad PA, Ødegård Ø, Candeloro M, Nornes SM, Malmquist C et al (2015) Underwater vehicles for environmental management in coastal areas. In: *OCEANS 2015-Genova*, IEEE, pp. 1–6
83. Dierssen HM, Zimmerman RC, Leathers RA, Downes TV, Davis CO (2003) Ocean color remote sensing of seagrass and bathymetry in the bahamas banks by high-resolution airborne imagery. *Limnol Oceanogr* 48(1part2):444–455
84. Mobley CD, Sundman LK, Davis CO, Bowles JH, Downes TV, Leathers RA, Montes MJ, Bissett WP, Kohler DD, Reid RP et al (2005) Interpretation of hyperspectral remote-sensing imagery by spectrum matching and look-up tables. *Appl Opt* 44(17):3576–3592
85. Volent Z, Johnsen G, Sigernes F (2007) Kelp forest mapping by use of airborne hyperspectral imager. *J Appl Remote Sens* 1(1):011503
86. Johnsen G, Ludvigsen M, Sørensen A, Aas LMS (2016) The use of underwater hyperspectral imaging deployed on remotely operated vehicles-methods and applications. *IFAC PapersOnLine* 49(23):476–481
87. Johnsen G, Volent Z, Dierssen H, Pettersen R, Ardelan M, Soreide F, Fearn P, Ludvigsen M, Moline M (2013) Underwater hyperspectral imagery to create biogeochemical maps of seafloor properties. In: J. Watson, O. Zielinski (eds) *Subsea Optics and Imaging*, Woodhead Publishing Series in Electronic and Optical Materials, pp. 508 – 540e. Woodhead Publishing. <https://doi.org/10.1533/9780857093523.3.508>
88. Ødegård Ø, Sørensen AJ, Hansen RE, Ludvigsen M (2016) A new method for underwater archaeological surveying using sensors and unmanned platforms. *IFAC-PapersOnLine* 49(23):486–493
89. Dumke I, Nornes SM, Purser A, Marcon Y, Ludvigsen M, Ellefmo SL, Johnsen G, Søreide F (2018) First hyperspectral imaging survey of the deep seafloor: high-resolution mapping of manganese nodules. *Remote Sens Environ* 209:19–30
90. McLeod D, Jacobson J, Hardy M, Embry C (2013) Autonomous inspection using an underwater 3d lidar. In: *Oceans-San Diego*, 2013, pp. 1–8. IEEE
91. Ozog P, Troni G, Kaess M, Eustice RM, Johnson-Roberson M (2015) Building 3d mosaics from an autonomous underwater vehicle, doppler velocity log, and 2d imaging sonar. In: *Robotics and Automation (ICRA), 2015 IEEE International Conference on*, pp. 1137–1143. IEEE



**Vaibhav Lodhi** received his B.E. in electronics and communication engineering, M. Tech in spatial information technology and currently pursuing PhD in hyperspectral imaging from Advanced Technology Development Center, IIT Kharagpur, India.



**Debashish Chakravarty** is a Professor in the Department of Mining Engineering, IIT Kharagpur, India. He worked as a postdoctoral research associate at Forschungszentrum Jlich GmbH, Germany. He was a recipient of the German Government Fellowship

for Postdoctoral Research in 2001. His research areas are mine mapping and localization, digital photogrammetry and geo-informatics.



**Pabitra Mitra** is a Professor in the Department of Computer Science and Engineering, IIT, Kharagpur, India. He received his doctorate from Indian Statistical Institute, Calcutta, India. His research areas are Machine Learning, Data Mining and Information Retrieval.